CHINESE OPTICS LETTERS

Vol. 19, No. 12 | December 2021

Wave mixing and high-harmonic generation enhancement by a two-color field driven dielectric metasurface [Invited]

Weifeng Yang (杨玮枫)[1,2,3*], Yichong Lin (林奕崇)[2], Xueyi Chen (陈雪仪)[2], Yuxuan Xu (徐雨萱)[2], Hongdan Zhang (张宏丹)[2,3], Marcelo Ciappina[4,5], and Xiaohong Song (宋晓红)[1,2,3**]

[1] School of Science, Hainan University, Haikou 570228, China

[2] Research Center for Advanced Optics and Photoelectronics, Department of Physics, College of Science, Shantou University, Shantou 515063, China

[3] Institute of Mathematics, Shantou University, Shantou 515063, China

[4] Physics Program, Guangdong Technion - Israel Institute of Technology, Shantou 515063, China

[5] Technion - Israel Institute of Technology, Haifa 32000, Israel

*Corresponding author: weifeng_yang@yeah.net

**Corresponding author: song_xiaohong@yeah.net

Received July 24, 2021 | Accepted September 14, 2021 | Posted Online October 15, 2021

High-harmonic generation in metasurfaces, driven by strong laser fields, has been widely studied. Compared to plasma, all-dielectric nanoscale metasurfaces possess larger nonlinearity response and higher damage threshold. Additionally, it can strongly localize the driven field, greatly enhancing its peak amplitude. In this work, we adopt a Fano resonant micro-nano structure with transmission peaks at different wavelengths and explore its nonlinear response by both single and two-color pump fields. Compared to the high-order harmonics induced by the first resonant wavelength, the intensity of the high-harmonic radiation results is enhanced by one order of magnitude, when the metasurface is driven by various resonant and non-resonant wavelength combinations of a two-color field.

Keywords: metamaterial; nanostructure; Fano resonance; high-harmonic generation; two-color field.
DOI: 10.3788/COL202119.123202

1. Introduction

High-harmonic generation (HHG) was firstly, to the best of our knowledge, proved to exist in rare-gas atoms[1], and nowadays it is one of the backbones of attosecond science[2–5]. Typical gas-phase HHG experiments need expensive and complex experimental setups. In recent years, solid materials have been extensively used as a driven medium for HHG. One of their advantages is its high density, typically three orders of magnitude larger, allowing the HHG to happen with lower pumping laser fields[6]. Thus, solid HHG has become a subject of great interest. Investigations have shown that high harmonics generated in bulk crystals could provide new ways to manipulate and tailor light fields and have instrumental prospects for strong field photonics applications[7–14]. These studies will pave the way to the design of compact ultrafast and short wavelength tunable coherent light sources. Subsequent research has shown that high-order harmonics can be generated in an engineered nanoscale structure, which is able to adequately tailor the local near-field in order to reach the strong field regime. Enhancing the driving electric field by a nanostructure is the most promising way to boost the interaction between the electromagnetic field and the material, allowing it to reach the strong laser–matter interaction, with lower intensity pumping fields.

Plasmonic-enhanced HHG studies have been triggered by the work of Kim *et al.*[15]. Even when the results of this work were still under debate, it sparked a large amount of both theoretical and experimental works[15–25]. Having the drawbacks of the seminal Kim's experiment in consideration and in order to obtain a higher conversion efficiency for HHG, we need to seek other alternative targets because, for instance, the incoherent plasma line emission cannot be ignored. In this way, solid materials appear as an attractive alternative. The inherent nonlinearity of dielectrics is, however, very difficult to exploit because the field enhancement always exists at sharp structure edges. Additionally, the enhanced field, able to trigger a strong nonlinear process, is only present on the surface of the nanostructure and rapidly decays as we move towards the bulk. Finally, plasmonics nanostructures have a large optical absorption and low melting point, which results in a low damage threshold, preventing the use of high laser peak strengths[26,27].

Therefore, high-refractive-index dielectric metasurfaces, exhibiting resonances in the optical domain, are one of the best alternative materials to enhance HHG[28,29]. This is due to its

large quality factors and high optical damage threshold[30–32]. Under resonant strong field conditions, the metasurface robustness can enrich the strong field mechanisms[33]. Furthermore, by using nanoscale films, it is possible to tailor the resonance-induced electromagnetic field enhancement. The geometry of each individual nanostructure appears as an instrumental feature for the HHG conversion efficiency. Moreover, the combination of different geometric shapes has great influence on it. It was both experimentally and theoretically verified that Si-based metasurfaces, supporting the electromagnetically induced transparency (EIT) effect, possess a large nonlinearity, which can greatly enhance the frequency conversion in the spectral region of the resonance[34–40].

Most of the studies based on dielectric metasurfaces focus on the monochromatic field excitation at the wavelength of its biggest transmittance. However, to the best of our knowledge, only a few works have studied the response of a two-color exciting field on the high-order harmonics generated by the metasurfaces[41–44]. In atomic systems, the efficiency of HHG can be significantly enhanced by adding a second color[45]. However, in dielectric metasurfaces, typically the driven light field is tuned at their resonant wavelength, so it appears attractive to explore whether the same gas-phase behavior can be observed in this new arena[46,47].

In this paper, we report both the difference frequency generation and high-order harmonic generation enhancement by using a combination of two different pump frequencies. The driven target is an all-dielectric nanostructure, and our research is motivated by the work of Ref. [48]. We demonstrate that, when the metasurface is excited by a combination of its first (λ_1) and second (λ_2) resonant wavelength fields, it generates an enhanced spectrum, with respect to the one obtained when only the first resonance frequency field drives the metasurface, with peaks at both the odd harmonics of the resonant frequency $(2m+1)\omega_1$, with m as an integer, and frequencies $(2m+1)\omega_1 \pm n(\omega_1-\omega_2)$, with n also as an integer. When the metasurface is excited by the mixture of its first resonant frequency field and its third harmonic, the spectrum generated, formed by an odd harmonic frequency comb, is enhanced more than one order of magnitude.

2. Simulations and Results

The simulation method is based on the finite-difference time-domain (FDTD) method, which is a method to obtain the time evolution of electromagnetic waves by solving the Maxwell curl equation in a finite spatial grid as originally proposed by Yee in 1966[49]. Establishing a time-discrete progressive sequence and dividing the electromagnetic field into the grid form of Yee cells, the electric and magnetic fields are calculated iteratively by using the difference method in the time domain. This approach is widely used in the numerical modeling of both the linear and nonlinear laser–nanostructures interaction. In Fig. 1(a), we depict a sketch of an array of Si-based metasurfaces on a sapphire substrate. Since this arrangement forms a periodic

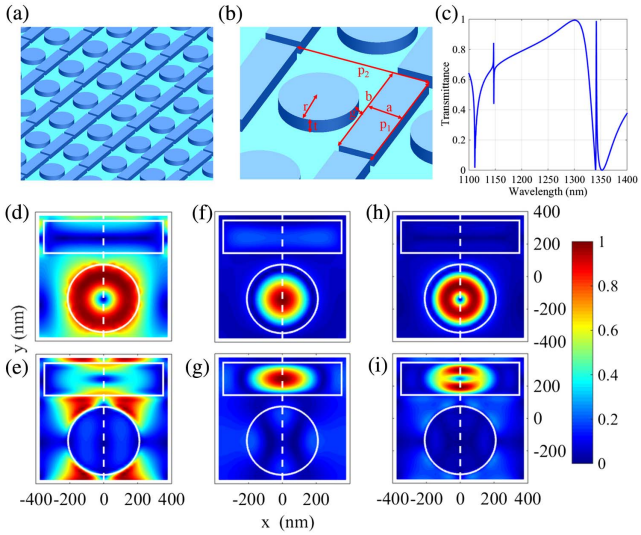

Fig. 1. (a) Scheme of the Si-based metasurface periodic arrangement on a sapphire substrate. (b) A single simulation cell. The geometrical parameters are a = 200 nm, b = 700 nm, r = 210 nm, g = 70 nm, t = 120 nm, P_1 = 750 nm, and P_2 = 750 nm. (c) Simulated transmittance spectrum of the single cell. One peak in the transmittance spectrum appears at a wavelength of 1341 nm, and another one is observed at a wavelength of 1146 nm. (d), (f), (h) Plots in the x–y plane of the electric, magnetic, and Poynting field patterns at a wavelength of 1341 nm, respectively. (e), (g), (i) Plots in the x–y plane of the electric, magnetic, and Poynting field patterns at a wavelength of 1146 nm, respectively. The white lines indicate the location of the nanostructures.

structure, we can select a single cell, formed by a dipolar bar antenna and a disk resonator, for our theoretical simulations [see Fig. 1(b)]. It is known that this type of structure hosts a Fano-like resonance, resulting in a classical analogue of the EIT effect[34]. Thus, the set of parameters results in $a = 200$ nm, $b = 700$ nm, $r = 210$ nm, $g = 70$ nm, $t = 120$ nm, $P_1 = 750$ nm, and $P_2 = 750$ nm[48]. Due to the fact that polycrystalline Si possesses both a large linear refractive index and a large nonlinear index in the near-infrared band, it is the material chosen for the bar antenna. Every single cell can then be strongly coupled to the external excitation driving it along a direction parallel to the bar, which supports the so-called 'bright' electric dipole resonance. The disk resonator, on the other hand, supports the so-called 'dark' magnetic dipole resonance, which cannot be excited directly by the incident light, but it can be excited by the near-field interaction with the bright mode.

We use a commercial software (Lumerical), based on the FDTD method[50], to numerically simulate the nonlinear optical response of the structure shown in Fig. 1(b). The pump laser beam falls perpendicular to the x–y plane of the Si-based metasurface, with its electric field linearly polarized along the bar. The electric field peak amplitude is set to be 1.55×10^8 V/m, corresponding to a peak pump intensity of 3.2 GW/cm^2, well below the material damage threshold, and the pulse length is 250 fs[48]. Figure 1(c) shows the theoretically simulated transmittance spectrum of the Si metasurface. From this curve, we can observe two sharp peaks, one located at a wavelength

$\lambda_1 = 1341$ nm, showing an EIT-like feature (we name this λ_1, the first resonant wavelength) and the other one at 1146 nm that we call the second resonant wavelength λ_2. The interference of the broadband 'bright' mode and narrowband 'dark' mode forms a typical three-level Fano resonant system[51,52]. The broadband absorption corresponds to the excitation of the metasurface bright mode. On the other hand, the sharp EIT peak is linked to the dark mode of the disk. Moreover, the second resonant wavelength λ_2 peak structure indeed resembles a Fano resonance. A Fano resonance results from the interference of a discrete auto-ionized state with a continuum state and gives rise to characteristically asymmetric peaks in the excitation spectrum[53–56]. In our scattering system, the transmission is strongly suppressed in a short frequency band and shows an asymmetric structure [see Fig. 1(c)].

Unlike most of the studies, we will focus not only on the nonlinear response of the system to the first resonant wavelength λ_1, but also pay attention to the contribution of the second resonant wavelength λ_2 in the resulting high-order harmonic generation. Therefore, let us first look at the spatial distribution of the electric, magnetic, and Poynting vector fields, both at the first and second resonant wavelengths. The results are shown in Figs. 1(d)–1(i). Figures 1(d), 1(f), and 1(h) show the electric, magnetic, and Poynting vector field patterns, respectively, at the first resonance wavelength $\lambda_1 = 1341$ nm. We can clearly observe that the three fields are strongly localized at the disk, while they vanish at the bar. A clear enhancement of the incoming peak amplitudes of the three fields can be extracted as well. For instance, the electric field is enhanced by a factor of 25–30 with respect to the incoming one, corresponding to around three orders of magnitude enhancement in the pumping intensity.

However, the distribution at the second resonance wavelength $\lambda_2 = 1146$ nm looks very different. Here, the electric field is not localized at either of the two nanostructures, but it presents maxima both at the gap between the nanostructures and the surrounding region of the disk and the bar [see Fig. 1(e)]. The magnetic and Poynting vector fields, on the contrary, are indeed strongly localized, as in the case of λ_1, but now at the bar [see Figs. 1(g) and 1(i)].

For this case, we also observe a substantial increase in the peak amplitudes of the three fields. We, then, conclude that the system should respond differently when it is excited by a laser pump centered at the first or the second resonance wavelength. Furthermore, we expect a dissimilar response as well when the metasurface is driven by combination of a two-color pulse, centered at different frequencies.

It was demonstrated that the excitation of resonant modes is one of the HHG enhancement mechanisms[57]. In the present work, however, we present other ways to improve the HHG efficiency, by going beyond the single-color resonant pumping. In this way, we explore the behavior of the metasurface under the excitation of different combinations of a two-color laser pump. As can be seen in Fig. 2(a), odd harmonics, visible up to the ninth order, are produced when the system is driven by a single-color laser pulse, spectrally centered at the first resonance frequency ω_1. Compared with the case of a single-color

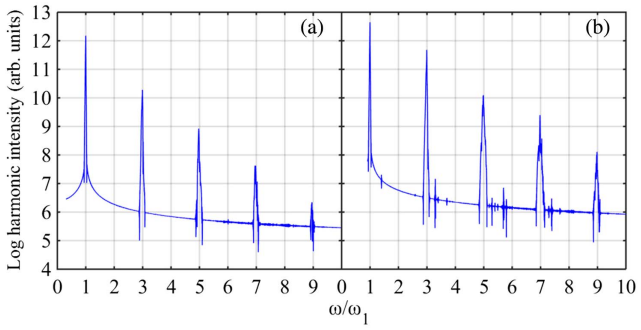

Fig. 2. (a) Harmonic spectrum when the excitation pulse is centered at the first resonance wavelength λ_1 = 1341 nm. (b) Harmonic spectrum when the excitation is a two-color field, formed by the combination of the resonant EIT wavelength (1341 nm) and its third harmonic. In both cases, the field is linearly polarized along the bar.

laser pump, the ninth harmonic still has a higher intensity. Furthermore, the intensity of the third harmonic is 1/100 weaker than that of the fundamental field. This trend seems to be followed by the rest of the harmonics. On the other hand, when the metasurface is excited by a combination of two frequencies, for the case of Fig. 2(b), the first resonance frequency and its third harmonic, the whole spectrum shows an enhancement of one order of magnitude.

In order to fully study the influence of a two-color incident field with different frequency combinations on the HHG, in Fig. 3, we use a laser pulse formed by the first and second resonant wavelengths λ_1 and λ_2. Additionally, as shown in the inset of Fig. 3, we show a zoom of the 1st, 3rd, and 5th harmonic

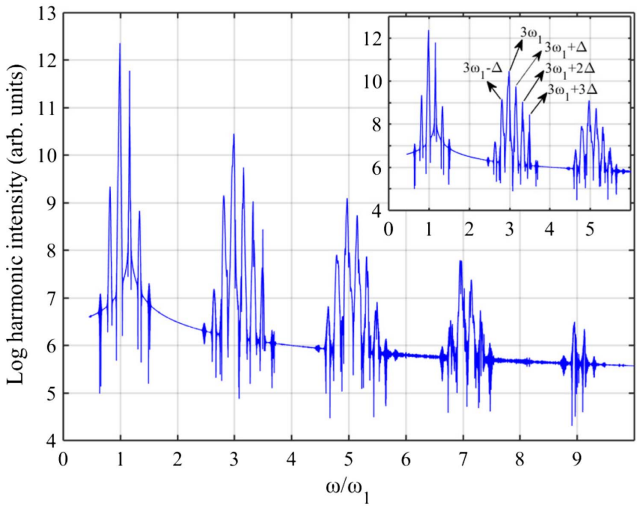

Fig. 3. Spectrum generated when the excitation pulse is a combination of the first resonance (resonant EIT peak) and the second resonance (1146 nm) wavelengths. The inset shows the zoom of the 1st, 3rd, and 5th harmonics of the spectrum. We label the additional frequencies around the third harmonic (see the text for more details). The driving field is linearly polarized along the bar.

orders, in order to further elucidate the positions of the additional harmonic frequencies.

Here, we observe a completely different behavior. Firstly, the harmonic intensity does not change compared to the one obtained when the metasurface is driven by a single-color field centered at the resonant frequency ω_1 [compare Figs. 2(a) and 3]. Secondly, additional spectral lines appear, i.e., at the peak of each odd harmonic of the resonant frequency ω_1, new peaks above and below its value are visible. For the case of Fig. 3, they are separated by an integer number of the frequency difference, i.e., $\pm n\Delta$, where $\Delta = (\omega_1 - \omega_2)$ (see the inset of Fig. 3 for the case of the third harmonic) and are a result of the wave mixing.

In nanostructures, the near-field is a delayed and enhanced "copy" of the excitation source. This delay can be experimentally measured and can give information about both the electron dynamics and tunneling time delay[58–61]. In order to study this phenomenon in our setup, we examine the modulation of the third-harmonic generation by the relative phase of the third frequency field, as shown in Fig. 4. When the amplitude of the third frequency field is 0.3 times that of the fundamental frequency field and the relative phase is between -2π and 2π, the third harmonic intensity shows a cos-type behavior. Additionally, the position of the first maximum has a 0.2π delay (zero delay corresponds to the situation when both fields are applied simultaneously), which corresponds to a time delay of 447.3 as. This value seems to be comparable with the one obtained in Ref. [58] for a gold nanotip.

Figure 5(a) shows the simulated transmittance spectrum of the metasurface with these new geometrical parameters. We can see now an EIT transmission peak at a wavelength of 800 nm, which we call first resonance wavelength λ_3, and another sharp one at a wavelength of 704 nm, which defines the second resonant wavelength λ_4. When we explore the distribution of the electric field, we found that the electric field is greatly enhanced at $\lambda_3 = 800$ nm, and it perfectly localizes inside the disk [see Fig. 5(b)]. This behavior is analogous to the one observed in Fig. 2(d). We also notice that the enhanced field covers a much

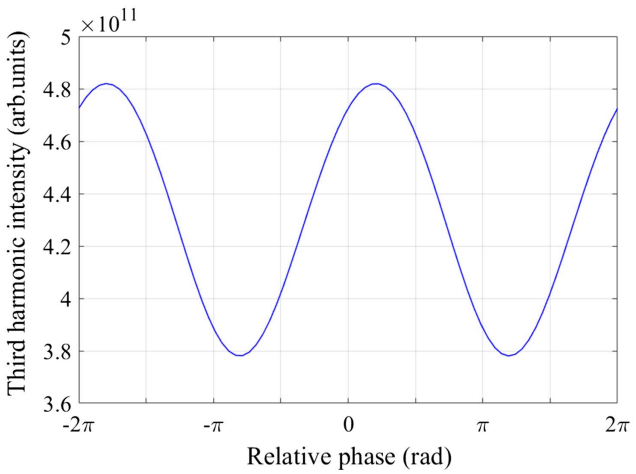

Fig. 4. Relation between the relative phase of the triple frequency field and the third harmonic intensity.

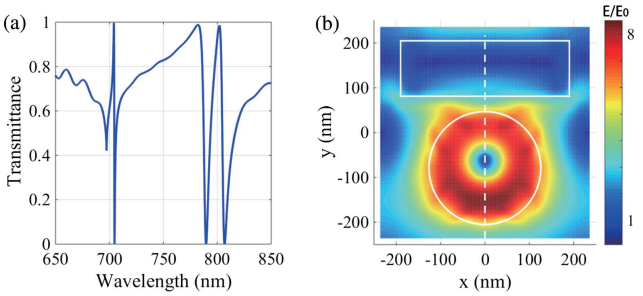

Fig. 5. (a) Simulated transmittance spectrum of the metasurface with the new geometrical parameters (see the text for details). (b) Simulated normalized electric field amplitude at the resonant wavelength λ_3 = 800 nm in the *x*–*y* plane. The white lines indicate the location of the nanostructures.

larger zone inside the disk, as compared with the previous case, although the enhanced factor is smaller.

To verify that the above results are not numerical artifacts, we further study the harmonic generation by changing the geometrical parameters of the nanostructure. In this way, we could make the metasurface have the Fano resonance at a different wavelength. For instance, if we require the metasurface to support the Fano-like resonance at 800 nm, the geometric parameters should be $a = 124$ nm, $b = 380$ nm, $r = 126$ nm, $g = 34$ nm, $t = 70$ nm, and $P_1 = P_2 = 470$ nm.

In order to study the nonlinear response of this new metasurface, we carry out simulations as in the previous case, i.e., we consider the nonlinear response in the all-dielectric nanostructure as excited by both a monochromatic laser pulse centered at the resonant wavelength λ_3 and different combinations of two-color laser pulses. Figure 6(a) shows the high-order harmonics resulting from the excitation by a monochromatic pumping field centered at λ_3. Here, only odd-order harmonics are observed. Similarly, when the target is driven by a two-color laser pulse formed by the first resonant wavelength λ_3 and its third harmonic, the HHG spectrum is now enhanced by one order of magnitude compared with the monochromatic case [see Fig. 6(b)].

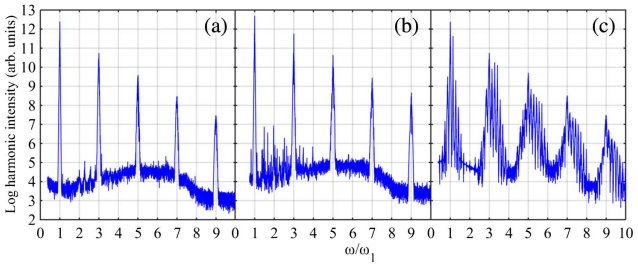

Fig. 6. (a) HHG for an excitation light pulse centered at 800 nm. (b) Two-color HHG spectrum for an incident field formed as a combination of the resonant frequency ω_3 and its third harmonic. (c) Wave mixing spectrum generated by an excitation pulse formed as the combination of the first and second resonant wavelengths λ_3 and λ_4. In all cases, the field is linearly polarized along the bar.

Finally, we pump the metasurface with a two-color laser field formed as the combination of the first and second resonant frequencies ω_3 and ω_4. The resulting spectrum can be observed in Fig. 6(c). Here, we see that, in addition to the odd-harmonic orders, new frequencies around each harmonic are present. It can be shown that these new peaks follow the formula $\pm n(\omega_3 - \omega_4)$. This result is identical to the one obtained for the previous case (see Fig. 3). Similarly, a marked yield enhancement compared to the monochromatic case of Fig. 5(a) is noticed. We can conclude thus, that the HHG spectra generated by a two-color pumping field are different from those excited by a single-color one, because of either an evident enhancement of all harmonic orders or the appearance of new peaks whose positions result from the wave mixing between the two driven laser sources frequencies.

3. Conclusions

We study the nonlinear response of a Fano resonant Si-based metasurface when driven by a strong laser field. We report an enhancement both in the high-harmonic emission as well as in the difference frequency generation. We demonstrate that if a two-color pump field is a mixture between the first resonant Si-metasurface frequency and its third harmonic, the whole HHG spectrum increases one order of magnitude. Additionally, if the driven field is a combination between the first and second resonant wavelengths, not only an enhancement in the whole HHG yield is observed but also new peaks appear. The positions of these peaks can be easily calculated from $\pm n\Delta$, where Δ is the difference between the pumping frequencies. The response of the Fano resonant Si-based metasurface appears to be robust against the changes in the geometrical parameters. Our work could pave the way for the design and potential realization of novel sources of tunable coherent light.

Acknowledgement

The work was supported by the National Natural Science Foundation of China (Nos. 11774215, 91950101, and 12074240), Sino-German Mobility Programme (No. M-0031), Department of Education of Guangdong Province (No. 2018KCXTD011), High Level University Projects of Guangdong Province (Mathematics, Shantou University), and Open Fund of the State Key Laboratory of High Field Laser Physics (SIOM).

References

1. M. Ferray, A. L'Huillier, X. Li, L. Lompré, G. Mainfray, and C. Manus, "Multiple-harmonic conversion of 1064 nm radiation in rare gases," J. Phys. B **21**, L31 (1988).
2. M. Ciappina, J. Pérez-Hernández, A. Landsman, W. Okell, S. Zherebtsov, B. Förg, J. Schötz, L. Seiffert, T. Fennel, T. Shaaran, T. Zimmermann, A. Chacón, R. Guichard, A. Zaïr, J. Tisch, J. Marangos, T. Witting, A. Braun, S. Maier, L. Roso, M. Krüger, P. Hommelhoff, M. Kling, F. Krausz, and M. Lewenstein, "Attosecond physics at the nanoscale," Rep. Prog. Phys. **80**, 054401 (2017).
3. G. Vampa, H. Fattahi, J. Vučković, and F. Krausz, "Nonlinear optics: attosecond nanophotonics," Nat. Photon. **11**, 210 (2017).
4. W. Yang, S. Gong, R. Li, and Z. Xu, "Generation of attosecond pulses in a system with permanent dipole moment," Phys. Lett. A **362**, 37 (2007).
5. H. Zhang, X. Liu, M. Zhu, S. Yang, W. Dong, X. Song, and W. Yang, "Coherent control of high harmonic generation driven by metal nanotip photoemission," Chin. Phys. Lett. **38**, 063201 (2021).
6. X. Song, S. Yang, R. Zuo, T. Meier, and W. Yang, "Enhanced high-order harmonic generation in semiconductors by excitation with multicolor pulses," Phys. Rev. A **101**, 033410 (2020).
7. S. Ghimire, A. Dichiara, E. Sistrunk, P. Agostini, L. Dimauro, and D. Reis, "Observation of high-order harmonic generation in a bulk crystal," Nat. Phys. **7**, 138 (2011).
8. T. Luu, M. Garg, S. Kruchinin, A. Moulet, M. Hassan, and E. Goulielmakis, "Extreme ultraviolet high-harmonic spectroscopy of solids," Nature **521**, 498 (2015).
9. G. Ndabashimiye, S. Ghimire, M. Wu, D. Browne, K. Schafer, M. Gaarde, and D. Reis, "Solid-state harmonics beyond the atomic limit," Nature **534**, 520 (2016).
10. H. Liu, Y. Li, Y. You, S. Ghimire, T. Heinz, and D. Reis, "High-harmonic generation from an atomically thin semiconductor," Nat. Phys. **13**, 262 (2016).
11. Y. You, D. Reis, and S. Ghimire, "Anisotropic high-harmonic generation in bulk crystals," Nat. Phys. **13**, 345 (2017).
12. S. Ghimire and D. Reis, "High-harmonic generation from solids," Nat. Phys. **15**, 10 (2019).
13. W. Yang, X. Song, S. Gong, Y. Cheng, and Z. Xu, "Carrier-envelope phase dependence of few-cycle ultrashort laser pulse propagation in a polar molecule medium," Phys. Rev. Lett. **99**, 133602 (2007).
14. X. Song, W. Yang, Z. Zeng, R. Li, and Z. Xu, "Unipolar half-cycle pulse generation in asymmetrical media with a periodic subwavelength structure," Phys. Rev. A **82**, 053821 (2010).
15. S. Kim, J. Jin, Y. Kim, I. Park, Y. Kim, and S. Kim, "High harmonic generation by resonant plasmon field enhancement," Nature **453**, 757 (2008).
16. M. Kauranen and V. Zayzts, "Nonlinear plasmonics," Nat. Photon. **6**, 737 (2012).
17. M. Klein, C. Enkrich, M. Wegener, and S. Linden, "Second-harmonic generation from magnetic metamaterials," Science **313**, 502 (2006).
18. B. Metzger, T. Schumacher, M. Hentschel, and M. Lippitz, "Third harmonic mechanism in complex plasmonic Fano structures," ACS Photon. **1**, 471 (2014).
19. J. Lassiter, X. Chen, X. Liu, T. Hoang, S. Oh, M. Mikkelsen, and D. Smith, "Third-harmonic generation enhancement by film-coupled plasmonic stripe resonators," ACS Photon. **1**, 1212 (2014).
20. J. Lee, M. Tymchenko, C. Argyropoulos, P. Chen, F. Lu, F. Demmerle, G. Boehm, M. Amann, A. AlÃź, and M. Belkin, "Giant nonlinear response from plasmonic metasurfaces coupled to intersubband transitions," Nature **511**, 65 (2014).
21. G. Vampa, B. Ghamsari, S. Siadat Mousavi, T. Hammond, A. Olivieri, E. Lisicka-Skrek, A. Yu Naumov, D. Villeneuve, A. Staudte, P. Berini, and P. Corkum, "Plasmon-enhanced high-harmonic generation from silicon," Nat. Phys. **13**, 659 (2017).
22. S. Han, H. Kim, Y. Kim, Y. Kim, S. Kim, I. Park, and S. Kim, "High-harmonic generation by field enhanced femtosecond pulses in metal-sapphire nanostructure," Nat. Commun. **7**, 13105 (2016).
23. M. Stockman, "Nanoplasmonics: the physics behind the applications," Phys. Today **64**, 39 (2011).
24. X. Song, S. Gong, W. Yang, S. Jin, X. Feng, and Z. Xu, "Coherent control of spectra effects with chirped femtosecond laser pulse," Opt. Commun. **236**, 151 (2004).
25. R. Zuo, X. Song, X. Liu, S. Yang, and W. Yang, "The influence of intraband motion on the interband excitation and high harmonic generation," Chin. Phys. B **28**, 094208 (2019).
26. X. Song, N. Wang, M. Yang, L. Cheng, J. Förstner, and W. Yang, "Direction-tunable enhanced emission from a wavelength metallic double-nanoslit structure," Opt. Express **25**, 13207 (2017).
27. D. Gramotnev and S. Bozhevolnyi, "Plasmonics beyond the diffraction limit," Nat. Photon. **4**, 83 (2010).

28. M. Semmlinger, M. Zhang, M. L. Tseng, T. T. Huang, J. Yang, D. P. Tsai, P. Nordlander, and N. J. Halas, "Generating third harmonic vacuum ultraviolet light with a TiO_2 metasurface," Nano Lett. **19**, 8972 (2019).
29. M. Semmlinger, M. L. Tseng, J. Yang, M. Zhang, C. Zhang, W. Y. Tai, D. P. Tsai, P. Nordlander, and N. J. Halas, "Vacuum ultraviolet light-generating metasurface," Nano Lett. **18**, 5738 (2018).
30. S. Liu, M. Sinclair, S. Saravi, G. Keeler, Y. Yang, J. Reno, G. Peake, F. Setzpfandt, I. Staude, T. Pertsch, and I. Brener, "Resonantly enhanced second-harmonic generation using III-V semiconductor all-dielectric metasurfaces," Nano Lett. **16**, 5426 (2016).
31. M. Shcherbakov, D. Neshev, B. Hopkins, A. Shorokhov, I. Staude, E. Melik-Gaykazyan, M. Decker, A. Ezhov, A. Miroshnichenko, I. Brener, A. Fedyanin, and Y. Kivshar, "Enhanced third-harmonic generation in silicon nanoparticles driven by magnetic response," Nano Lett. **14**, 6488 (2014).
32. G. Grinblat, Y. Li, M. Nielsen, R. Oulton, and S. Maier, "Enhanced third harmonic generation in single germanium nanodisks excited at the anapole mode," Nano Lett. **16**, 4635 (2016).
33. M. R. Shcherbakov, H. Zhang, M. Tripepi, G. Sartorello, N. Talisa, A. Alshafey, Z. Y. Fan, J. Twardowski, L. A. Krivitsky, A. I. Kuznetsov, E. Chowdhury, and G. Shvets, "Generation of even and odd high harmonics in resonant metasurfaces using single and multiple ultra-intense laser pulses," Nat. Commun. **12**, 4185 (2021).
34. S. Harris, "Electromagnetically induced transparency," Phys. Today **50**, 36 (1997).
35. Y. Yang, I. Kravchenko, D. Briggs, and J. Valentine, "All-dielectric metasurface analogue of electromagnetically induced transparency," Nat. Commun. **5**, 5753 (2014).
36. A. Kuznetsov, A. Miroshnichenko, M. Brongersma, Y. Kivshar, and B. L'yanchuk, "Optically resonant dielectric nanostructures," Science **354**, aag2472 (2016).
37. S. Jahani and Z. Jacob, "All-dielectric metamaterials," Nat. Nanotech. **11**, 23 (2016).
38. M. Limonov, M. Rybin, A. Poddubny, and Y. Kivshar, "Fano resonances in photonics," Nat. Photon. **11**, 543 (2017).
39. K. Boller, A. Imamolu, and S. Harris, "Observation of electromagnetically induced transparency," Phys. Rev. Lett. **66**, 2593 (1991).
40. B. Metzger, T. Schumacher, M. Hentschel, M. Hentschel, M. Lippitz, and H. Giessen, "Third harmonic mechanism in complex plasmonic Fano structures," ACS Photon. **1**, 471 (2014).
41. G. Grinblat, Y. Li, M. Nielsen, R. Oulton, and S. Maier, "Degenerate four-wave mixing in a multiresonant germanium nanodisk," ACS Photon. **4**, 2144 (2017).
42. S. Liu, P. Vabishchevich, A. Vaskin, J. Reno, G. Keeler, M. Sinclair, I. Staude, and I. Brener, "An all-dielectric metasurface as a broadband optical frequency mixer," Nat. Commun. **9**, 2507 (2018).
43. R. Colom, L. Xu, L. Marini, F. Bedu, I. Ozerov, T. Begou, J. Lumeau, A. Miroshnishenko, D. Neshev, B. Kuhlmey, S. Palomba, and N. Bonod, "Enhanced four-wave mixing in doubly resonant Si nanoresonators," ACS Photon. **6**, 1295 (2019).
44. X. Song, R. Zuo, S. Yang, P. Li, T. Meier, and W. Yang, "Attosecond temporal confinement of interband excitation by intraband motion," Opt. Express **27**, 2225 (2019).
45. S. Watanabe, K. Kondo, Y. Nabekawa, A. Sagisaka, and Y. Kobayashi, "Two-color phase control in tunneling ionization and harmonic generation by a strong laser field and its third harmonic," Phys. Rev. Lett. **73**, 2692 (1994).
46. X. Song, M. Wu, Z. Sheng, D. Dong, H. Wu, and W. Yang, "Carrier-envelope phase dependence of the half-cycle soliton generation in asymmetric media," Laser Phys. Lett. **11**, 056002 (2014).
47. X. Song, M. Yan, M. Wu, Z. Sheng, Z. Hao, C. Huang, and W. Yang, "Soliton frequency shifts in subwavelength structures," J. Opt. **17**, 055503 (2015).
48. Y. Yang, W. Wang, A. Boulesbaa, I. Kravchenko, D. Briggs, A. Puretzky, D. Geohegan, and J. Valentine, "Nonlinear Fano-reonant dielectric metasurfaces," Nano. Lett. **15**, 7388 (2015).
49. K. Yee, "Numerical solution of initial boundary value problems involving Maxwell's equations in isotropic media," IEEE Trans. Antennas Propag. **14**, 302 (1966).
50. https://www.lumerical.com/products
51. W. Yang, S. Gong, and Z. Xu, "Enhancement of ultrafast four-wave mixing in a polar molecule medium," Opt. Express **14**, 7216 (2006).
52. W. Yang, S. Gong, Y. Niu, S. Jin, and Z. Xu, "Enhancement of four-wave mixing induced by interacting dark resonances," J. Phys. B **38**, 2657 (2005).
53. A. Miroshnichenko, S. Flach, and Y. Kivshar, "Fano resonances in nanoscale structures," Rev. Mod. Phys. **82**, 2257 (2010).
54. M. Limonov, M. Rybin, A. Poddubny, and Y. Kivshar, "Fano resonances in photonics," Nat. Photon. **11**, 543 (2017).
55. W. Yang, X. Song, Z. Zeng, R. Li, and Z. Xu, "Quantum path interferences of electron trajectories in two-center molecules," Opt. Express **18**, 2558 (2010).
56. W. Yang, H. Zhang, C. Lin, J. Xu, Z. Sheng, X. Song, S. Hu, and J. Chen, "Momentum mapping of continuum electron wave packet interference," Phys. Rev. A **94**, 043419 (2016).
57. H. Liu, C. Guo, G. Vampa, J. Zhang, T. Sarmiento, M. Xiao, P. Bucksbaum, J. Vuckovic, S. Fan, and D. Reis, "Enhanced high-harmonic generation from an all-dielectric metasurface," Nat. Phys. **14**, 1006 (2018).
58. B. Förg, J. Schötz, F. Süßmann, M. Förster, M. Krüger, B. Ahn, W. Okell, K. Wintersperger, S. Zherebtsov, A. Guggenmos, V. Pervak, A. Kessel, S. Trushin, A. Azzeer, M. Stockman, D. Kim, F. Krausz, P. Hommelhoff, and M. Kling, "Attosecond nanoscale near-field sampling," Nat. Commun. **7**, 11717 (2016).
59. J. Schotz, B. Förg, M. Förster, W. Okell, M. Stockman, F. Krausz, P. Hommelhoff, and M. F. Kling, "Reconstruction of nanoscale near fields by attosecond streaking," IEEE J. Sel. Top. Quantum Electron. **23**, 8700111 (2016).
60. X. Gong, C. Lin, F. He, Q. Song, K. Lin, Q. Ji, W. Zhang, J. Ma, P. Lu, Y. Liu, H. Zeng, W. Yang, and J. Wu, "Energy-resolved ultrashort delays of photoelectron emission clocked by orthogonal two-color laser fields," Phys. Rev. Lett. **118**, 143203 (2017).
61. X. Song, G. Shi, G. Zhang, J. Xu, C. Lin, J. Chen, and W. Yang, "Attosecond time delay of retrapped resonant ionization," Phys. Rev. Lett. **121**, 103201 (2018).